

TECHNICAL DESIGN NOTE

Multi-pass light amplification for tomographic particle image velocimetry applications

Sina Ghaemi and Fulvio Scarano

Delft University of Technology, Faculty of Aerospace, Department of Aerodynamics, Kluyverweg 2, 2629HT, The Netherlands

E-mail: s.ghaemi@tudelft.nl

Received 20 August 2010, in final form 24 September 2010

Published 4 November 2010

Online at stacks.iop.org/MST/21/127002

Abstract

The light source budget is a critical issue for tomographic particle image velocimetry (Tomo-PIV) systems due to its requirement for large illuminated volume and imaging at small apertures. In this work, a light amplification system based on the multi-pass concept is investigated for Tomo-PIV applications. The system design is performed on the basis of a theoretical model providing an estimation of the most important system parameters and above all the amplification gain. The multi-pass light amplification concept is verified experimentally by measuring the scattered light intensity across the illuminated volume. The results demonstrate a gain factor of 7 and 5 times in comparison with the single-pass and double-pass illumination approaches, respectively.

Keywords: light amplification, laser, multi-pass reflection, tomographic PIV

(Some figures in this article are in colour only in the electronic version)

Introduction

The intensity level of the light source plays a crucial role in various laser-based measurement techniques. An incoming light of low intensity results in a low signal-to-noise ratio and consequently low measurement accuracy. This has strongly motivated researches to explore different methods for optimization/amplification of the light source budget in laser-based diagnostic systems.

Over the last few decades, the issue of light budget has especially been critical for measurement techniques such as Raman, Rayleigh and Thomson scattering as the scattered signal is significantly lower than the incidence light. Different methods such as multi-pass light amplification [1] have been sought in order to augment the light intensity at the measurement spot.

For techniques based on light scattering by particle tracers immersed in the flow, the issue of light source budget has

not been critical for methods based on point-wise (e.g. laser Doppler anemometry) or planar illumination (PIV, planar laser-induced fluorescence). Instead, Tomo-PIV (Elsinga *et al* [2]) involves at least an order of magnitude increase in the light source energy in comparison to planar PIV. Such an increase is due to two factors: (1) the measurement volume has a larger cross section (e.g., $80 \times 90 \times 20 \text{ mm}^3$, [3]) and (2) the particle tracers need to be imaged in-focus over a finite depth, requiring a high numerical aperture (e.g. f -number 22–32). Furthermore, the light source requirement becomes even more critical in high-speed Tomo-PIV since a few orders of magnitude higher power should be applied to sustain the required light intensity per laser pulse [4].

This work aims to investigate light amplification across a Tomo-PIV measurement volume using a multi-pass reflection technique. The approach was utilized in tomographic experiments for the measurement of turbulent boundary layer flows in air [4]. However, the design and optimization of

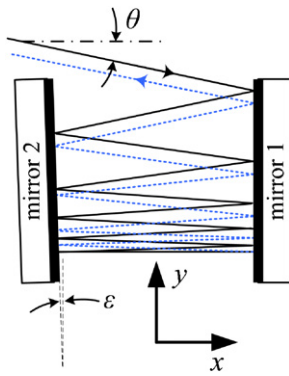


Figure 1. Schematic drawing of the multi-pass light amplification system. The path of the downward propagating light beam is in solid black and the upward propagating beam in dashed blue.

such system requires a detailed discussion of its characteristics and performances, which is proposed here. The amplification system can also be of interest for illuminating a volume for other measurement techniques such as 3D particle tracking velocimetry [5] and digital defocusing PIV [6]. The note provides a mathematical model based on geometrical optics, along with experimental details of the amplification system and estimation of the performance for configurations relevant to tomographic PIV experiments. Finally, the gain factor of the multi-pass amplification system is experimentally measured and compared with single-pass and double-pass illumination systems.

Multi-pass light amplification

As described in its first application to time-resolved Tomo-PIV experiment by Schröder *et al* [4], the multi-pass light

amplification system consists of two opposing mirrors in order to obtain multiple reflections of the light beam across the measurement volume. As shown in figure 1, the incoming light strikes mirror 1 at an angle θ while the two mirrors are placed at a small angle (ϵ) with respect to each other (mirror 1 is parallel to the y axis). As a result of ϵ , the angle of reflection of the laser beam gradually decreases as it travels downward between the mirrors (solid lines in the figure). The reflection angle eventually reverses and leads to a second sequence of upward reflections which guide the laser beam again through the illuminated volume toward the upper side (dashed lines in the figure) where it eventually exits the amplifier cell. The distance between two subsequent beams decreases toward the lower side of the mirrors. However, the intensity of the laser beam also reduces due to optical losses such as beam divergence, scattering by the particles and reflection loss along the transmission path. This maintains the same order of magnitude intensity along the y direction.

A general view of the multi-pass light amplification system along with the magnified view of specific regions is illustrated in figure 2. The laser beam of diameter d should be chosen according to the required height of the measurement volume, H . Because typically $d < H$, a beam expander, consisting of a negative/positive pair of spherical lenses, needs to be used. The lens combination can also control the beam diameter in order to maintain it constant along the total optical path, which is performed by adjusting the distance between the spherical lenses. The final beam diameter, d , should be selected slightly in excess of the height (i.e. $d \approx 1.2H$). The low intensity periphery of the laser beam (assuming a Gaussian distribution) should be cut out by knife-edge filters placed on the two mirrors (along the y axis). The beam enters at an angle $-\theta$ with respect to the x axis while the first mirror (M1) and the second mirror (M2) are at 0 and ϵ angle with respect to the y axis ($\epsilon \ll \theta$).

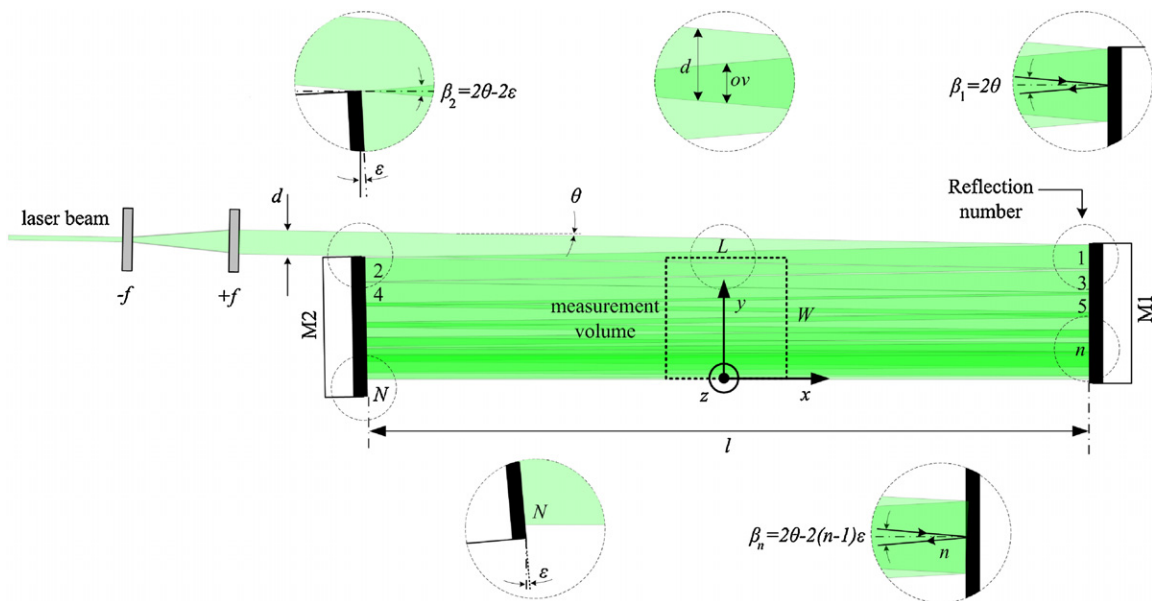


Figure 2. Schematic of the multi-pass light amplification setup showing the optical path of the laser beam along with the spherical lenses and the mirrors.

The laser beam reflected by M1 will form an angle $\beta_1 = 2\theta$ with respect to the incident beam at the first reflection. (The angle between the incident and the reflected light beams at the n th reflection is indicated by β_n .) This process is shown in the magnified view at the top right corner of figure 2. After this reflection, two important points must be considered as the reflected beam travels back toward the M2. First, as shown in the center-top detailed view of figure 2, the first reflected beam from M1 should have about 50% overlap with the initial beam (i.e. $ov = d/2$) at $x = 0$. In general, high overlap of the laser beams is desired to flatten the local minima observed along the y axis due to the laser beam intensity distribution. Second, the mirror M2 should not interfere with the initial beam and at the same time the reflected beam from M1 must be completely captured by M2. Consequently, M2 should be shifted down in the y direction by $l\theta$ with respect to the position of M1. At the optimized configuration, the two laser beams will be adjacent without any overlap or gap. These two criteria are satisfied if

$$\theta \approx \frac{d}{2l}. \quad (1)$$

In the case that the mirror coating does not reach the edge, the above equation needs to be modified by substituting d with $d + t$, where t is the length of the uncoated border of the mirror. It follows from equation (1) that an excessive expansion of the initial laser beam should be avoided, as it requires higher θ . It will be shown later that higher θ is not desirable since it results in the reduction of the number of reflections and the overlap between the laser beams.

At the first reflection from M2 ($n = 2$ in figure 2), the laser beam incidence angle is $(\theta - \varepsilon)$ and $\beta_2 = 2\theta - 2\varepsilon$. The angle β decreases by 2ε after each reflection and is expressed for the n th reflection by

$$\beta_n \approx 2\theta - 2(n - 1)\varepsilon. \quad (2)$$

Using equation (2) and noting that the laser beam will propagate upward if β becomes negative, the number of reflections of the laser beam in one sequence from the top to the bottom of the mirrors, N , can be related to θ and ε according to

$$N = \left\lfloor \frac{\theta}{\varepsilon} \right\rfloor - 1. \quad (3)$$

The number of reflections can be used to estimate the amplification gain (G) of the system in comparison to the initial laser beam as

$$G = 1 + \left(N - \frac{N(N+1)}{2} \tau \right), \quad (4)$$

where τ is the energy loss per pass due to reflection at the mirror and scatter by the seeding particles. Equation (4) has been linearized assuming $\tau \ll 1$. The width of the measurement volume (W) can be estimated using the sequence of β angles by

$$W = Nl\theta - N(N-1)\frac{l}{2}\varepsilon. \quad (5)$$

The experimental conditions impose W and l and equation (1) can be used to calculate θ . Therefore, N and ε can be evaluated from equations (3) and (5). The first term on the right-hand

Table 1. Examples of the design parameters in several light amplification experiments. d , l and W are selected based on the desired experiment. The gain (G) is calculated assuming 2% energy loss per pass.

Configuration	d (mm)	l (m)	W (mm)	θ (deg)	ε (deg)	N	G
1	10	0.5	50	0.573	0.030	18	15.6
2	10	1	50	0.287	0.015	18	15.6
3	20	0.5	50	1.146	0.120	8	8.3
4	20	0.5	100	1.146	0.060	18	15.6
5	20+2 ^a	0.6	50	1.050	0.131	7	7.4

^a The modification accounts for the uncoated edge of the mirror.

side of the latter equation corresponds to the case in which the two mirrors are parallel. The second term is the reduction in W due to the angle between the two mirrors, ε .

An evaluation of the above parameters is proposed in table 1, where the calculated values for θ , ε , N and G corresponding to four configurations are given. Configuration 1 serves as a basis for comparison while l and d are varied in configurations 2 and 3, respectively. In configuration 4, both d and W are varied to model a larger experimental setup. Configuration 5 corresponds to the current experimental setup, described in the next section. A comparison of configurations 1 and 2 shows that the increase in the distance between the two mirrors, l , does not affect the number of passes if achieving smaller angles is feasible in practice. It is also observed that the increase in the beam diameter in configuration 3 has reduced the number of passes of the laser beam, and consequently lower amplification gain can be theoretically obtained. The last configuration shows the effect of a higher measurement width, W . In comparison with configuration 3, smaller ε is required and a higher number of reflections is achieved. This table also provides the order of magnitude of the angles required for a multi-pass amplification system setup. For the configurations shown in table 1, ε should be adjusted at least within an accuracy of 0.01° . This also sets a limit on the structural vibration that such a system can tolerate, for instance when operating connected to rotating machinery or a wind tunnel.

Experimental verification

An experimental setup is developed to investigate the light intensity across a volume illuminated by the multi-pass light amplification technique. Single-pass and double-pass [3] illumination configurations are also considered here for comparison.

A photograph of the experimental setup is shown in figure 3, with the mirrors visible on the right and left sides of the image. Some smoke is introduced to visualize the illuminated region. The light source is a Quantronix *Darwin-Duo* Nd:YLF laser (2×25 mJ/pulse at 1 kHz). The initial light beam of 6 mm diameter is expanded to 18 mm using a positive ($f = 200$) and a negative ($f = -100$) spherical lens. The distance between the lens pair is adjusted in order to maintain a constant beam diameter along the optical transmission path.

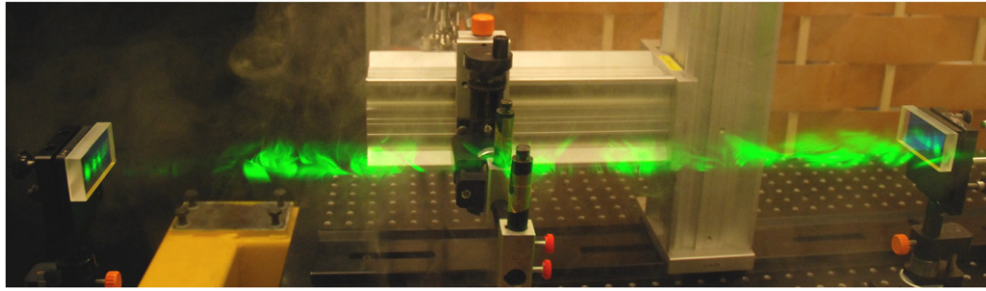


Figure 3. Light amplification system setup. The two mirrors are on the left and right sides. The structure in the middle supports the thin wire across the illuminated volume.

Two highly reflective rectangular mirrors from Laser Components GmbH of $30 \times 60 \text{ mm}^2$ are used to reflect the laser beam across the measurement volume. These mirrors have 2 mm of uncoated edge on each side of the longer dimension, which results in 56 mm of reflective length. The mirrors are mounted on high precision holders, equipped with micrometric screws in a brass bushing. The distance between the mirrors is $l = 60 \text{ cm}$. Such a distance is typically dictated by the flow facility (e.g., the span of the wind tunnel). In total the laser beam undergoes 12 passes ($N = 6$) across the illuminated volume which results in approximately 7 m of optical transmission path. Two pairs of knife-edge filters are also aligned with the longer sides of the mirrors in order to cut straight edges into the illuminated volume along the y axis. The theoretical performance of the system is given in table 1 (configuration 5). In this case, the length of the uncoated border of the mirror, t , is added to the laser beam diameter, d . The predictions yield $N = 7$ and $G = 7.4$.

In the single pass configuration the laser beam is expanded using $f = -100$ and 200 spherical lenses and stretched in the y direction using $f = -40$ cylindrical lens. The expanded laser beam has an elliptical cross-section with minor and major axes of 30 mm and 300 mm, respectively. The cross section of the expanded laser beam is larger than the desired measurement volume ($30 \times 60 \text{ mm}^2$). This is because the borders of the illuminated volume significantly suffer from low light intensity due to the initial Gaussian distribution of the laser beam, which is not acceptable. It is therefore necessary to over-expand the beam and only include its high-energy portion to avoid under-illuminated regions at the borders. For the double pass configuration, a mirror is placed after the measurement volume at $x = 50 \text{ mm}$ to reflect the expanded beam and obtain the second pass of the laser light across the same region. The effect of beam divergence after reflection is negligible due to the small 50 mm distance between the measurement volume and the mirror.

The illumination intensity is measured by means of a $50 \mu\text{m}$ diameter wire aligned along the y direction and placed at several positions along the height. The light scattered by the wire is recorded by a CMOS camera (LaVision GmbH, *HighSpeedStar 6*). The camera has a 12 bits sensor of 1024×1024 pixels and is equipped with a Nikon objective ($f = 105 \text{ mm}$) set at $f = 32$ to obtain focused images of the wire at several positions along the depth. The optical axis is aligned with the illuminated volume height and has

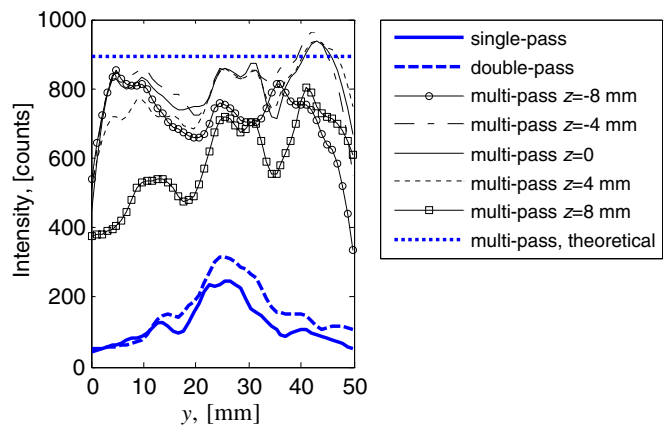


Figure 4. Scattered intensity by the wire across the illuminated volume.

a magnification factor of 0.4 and $50 \times 50 \text{ mm}^2$ field-of-view. It is important to note that the amount of collected light depends upon the observation angle of the camera. In this work, in order to obtain results of general validity and prevent any bias due to imaging configuration, the camera is placed perpendicular (side scatter) to the beam for all configurations, which yields a conservative estimation of the intensity level within the illuminated region.

Results

The results of the light intensity measurement across the illuminated volume for the single-pass, double-pass and multi-pass configurations are shown in figure 4 as light intensity (counts) detected by the camera versus the y axis for different z heights. It is observed that the single-pass configuration results in the lowest intensity level. There is a peak of 230 counts at $y = 25 \text{ mm}$, which is due to the initial Gaussian intensity distribution of the laser beam. The double-pass configuration results in about 25% increase of the peak intensity. The total light energy (based on the area beneath the plot) increases by 30% upon using the double-pass configuration. This low gain level is mainly due to further divergence, along the y direction, of the laser light after the first pass.

The light intensity corresponding to the multi-pass amplification in figure 4 shows an illumination intensity

increase of approximately seven times in comparison to the single-pass configuration. The intensity level is also relatively uniform along the illumination region height within the range $z = -4$ to $+4$ mm and it is still significantly higher than the single-pass configuration at $z = -8$ and $+8$ mm. This demonstrates the possibility of extending the measurement height from 8 up to 16 mm. The local peaks observed along the y direction correspond to the center of the reflected laser beams. To further homogenize the light intensity distribution one would need to increase the overlap factor between subsequent reflections, which can be achieved by decreasing the entrance angle θ . The amplification gain predicted by the theoretical model is also reported in figure 4. The comparison with the experimental results shows a slight overestimation of the amplification gain which can be due to further optical losses such as laser beam divergence.

Conclusion

The amplification of light intensity across a volume illuminated using the multi-pass light amplification system has been theoretically and experimentally investigated. A model is proposed to predict the main system parameters, such as the number of reflections, the angles of the laser beam and the mirrors, and the overall gain of the system. This model

provides design detail for light amplification cells in Tomo-PIV experiments. The concept is verified by an experiment and the amplification gain is determined and compared to single-pass and double-pass illumination systems. An amplification factor of 7 and 5 times is achieved in comparison to the single-pass and the double-pass configurations, respectively.

References

- [1] Santavicca D A 1979 A high energy, long pulse Nd:YAG laser multipass cell for Raman scattering diagnostics *Opt. Commun.* **30** 423–5
- [2] Elsinga G E, Scarano F, Wieneke B and van Oudheusden B W 2006 Tomographic particle image velocimetry *Exp. Fluids* **41** 933–47
- [3] Scarano F and Poelma C 2009 Three-dimensional vorticity patterns of cylinder wakes *Exp. Fluids* **47** 69–83
- [4] Schröder A, Geisler R, Elsinga G E, Scarano F and Dierksheide U 2008 Investigation of a turbulent spot and tripped turbulent boundary layer flow using time-resolved tomographic PIV *Exp. Fluids* **44** 305–16
- [5] Maas H G, Gruen A and Papantoniou D 1993 Particle tracking velocimetry in three-dimensional flows—part 1. Photogrammetric determination of particle coordinates *Exp. Fluids* **15** 133–46
- [6] Pereira F and Gharib M 2002 Defocusing digital particle image velocimetry and the three-dimensional characterization of two-phase flows *Meas. Sci. Technol.* **13** 683–94